Chapter 50
Development of Portable, Wireless and Smartphone Controllable Near-Infrared Spectroscopy System

Takashi Watanabe, Rui Sekine, Toshihiko Mizuno, and Mitsuharu Miwa

Abstract We have developed portable near-infrared tissue oxygenation monitoring systems, called the "PocketNIRS Duo" and the "PocketNIRS HM", which features wireless data communication and a sampling rate of up to 60 data readings per second. The systems can be controlled by smartphone or personal computer. We demonstrate the efficacy of the systems for monitoring changes in brain and arm muscle hemodynamics and oxygenation in breath-holding and cuff-occlusion tests, respectively.

Our systems should prove to be useful as an oxygenation monitor not only in research but also in healthcare applications.

Keywords Near-infrared spectroscopy (NIRS) • Oxygenation • Portable • Wireless • High sampling rate

1 Introduction

Near-infrared spectroscopy (NIRS) technologies are used for the non-invasive determination of the amount of absorbing molecular species in tissue, especially oxyhemoglobin and deoxyhemoglobin [1–5]. NIR light in the wavelength range of 700–1000 nm, which is called the "optical window for tissues", is able to penetrate

T. Watanabe (✉) • R. Sekine
Optical Diagnostic Technology Group, Development Center, Hamamatsu Photonics K.K., Hamamatsu, Japan
e-mail: tk-wat@crl.hpk.co.jp

T. Mizuno
DynaSense Inc., Hamamatsu, Japan

M. Miwa
Development Center, Hamamatsu Photonics K.K., Hamamatsu, Japan

Q. Luo et al. (eds.), *Oxygen Transport to Tissue XXXVIII*, Advances in Experimental Medicine and Biology 923, DOI 10.1007/978-3-319-38810-6_50

several centimeters into a variety of tissues because of the low absorbance of hemoglobin and water at these wavelengths. There are three fundamental approaches to measuring oxygenation in tissue non-invasively: the continuous wave (CW), frequency resolved and time resolved techniques. NIRS using CW is the simplest and most practical of these technologies, although it is difficult to acquire the absolute hemoglobin concentration with this method.

Several CW NIRS systems are commercially available. However, these systems exhibit poor portability owing to their size and weight, fragile optical fibers that are easy to break, and slow data acquisition rates, all of which can make their use inconvenient. We have developed a portable, fiber-free, battery-operated, low noise, highly sensitive, wireless NIRS system with a fast sampling rate and two-channel probe operation. The product is called the "PocketNIRS Duo". We expect that our wireless and portable NIRS system will prove to be a useful device in a number of fields including the healthcare industry, brain research, and brain–machine interfaces.

2 Instrumentation

2.1 PocketNIRS Duo

The PocketNIRS Duo consists of three main parts, as shown in Fig. 50.1: the optical probes, the controller, and the interface device (smartphone or personal computer). The optical probe has three built-in NIR light emitting diodes (LEDs) as light sources and a single silicon PIN photodiode as an optical detector which is positioned 3 cm from the LEDs. The analog signal from the photodiode is amplified and converted to a digital signal within the optical probe and then transferred to the

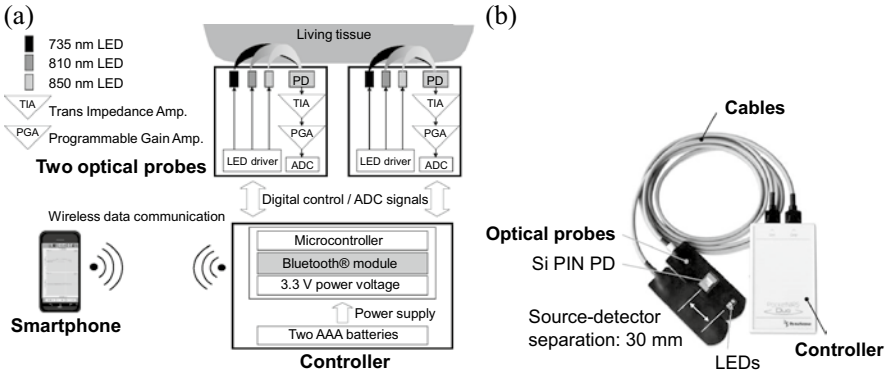

Fig. 50.1 Our wireless NIRS system "PocketNIRS Duo" (**a**) Schematic diagram (**b**) External view

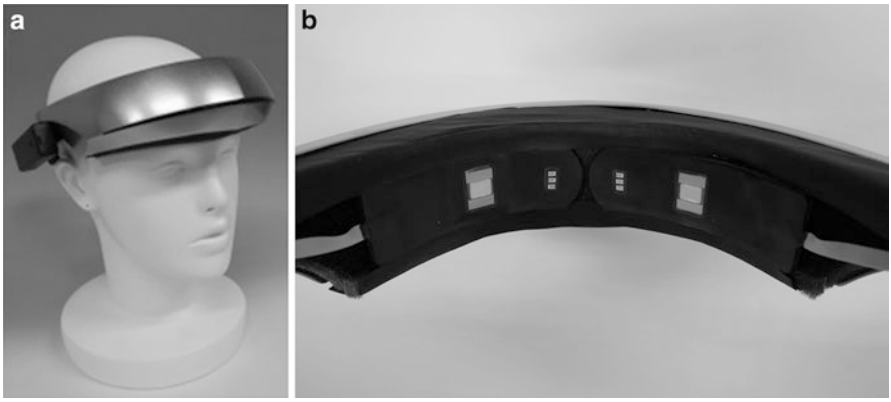

Fig. 50.2 PocketNIRS HM (**a**) External view (**b**) Internal view

controller via a 1 m long electrical cable. Digitization of the analogue signal prior to data transfer helps to preserve signal quality. The programmable gain amplifier (PGA) enables the measurement of signals over a wide dynamic range. The smartphone acquires and analyzes the data transmitted from the controller by Bluetooth® wireless technology, and then displays the results.

2.2 PocketNIRS HM

The PocketNIRS Duo has been designed for the analysis of oxygenation and hemodynamics in a number of tissues including brain and muscle.

The requirement for measuring the oxygenation state of the brain is increasing. We have therefore designed a variant of the PocketNIRS, the "PocketNIRS HM", specifically for the measurement of brain oxygenation (Fig. 50.2). All specifications are the same as those described for the PocketNIRS Duo. The control circuit, two optical probes, Bluetooth wireless data transmitter and battery are all integrated into a plastic helmet. This device does not require the use of double-sided tape on the optical probe. The PocketNIRS HM is simply mounted onto the head of the subject, the power turned on, and the start button on the smartphone pressed. The system then starts measurements immediately.

3 The Principles of the PocketNIRS Duo

The changes in tissue concentrations of oxyhemoglobin and deoxyhemoglobin can be determined using the modified Beer-Lambert law. When the NIR light sources illuminate a tissue, the photodetector receives backscattered photons from the tissue. The penetration depth of detection is approximately one half the distance

between the light sources and the photodetector. For example, if the light source and photodetector are separated by a distance of 3 cm, then the penetration depth is expected to be approximately 1.5 cm.

The attenuation of incident light intensity can be formulated as follows:

$$OD(\lambda,t) = \log_{10} \frac{I_{in}(\lambda,t)}{I_{out}(\lambda,t)} = A(\lambda,t) + S(\lambda,t), \tag{50.1}$$

where $I_{in}(\lambda, t)$ is the incident light intensity, $I_{out}(\lambda, t)$ is the detected intensity, and $OD(\lambda, t)$ is the optical density for wavelength λ at time t and is defined as the attenuation in light intensity as a function of the wavelength λ at time t. This attenuation can also be defined as the superposition of absorption $A(\lambda, t)$ and scattering $S(\lambda, t)$ of NIR light. Oxyhemoglobin and deoxyhemoglobin are the main absorbers of light in the NIR region in human tissue and their concentrations at a given point in time can be used to derive the light absorbance. Therefore, light absorbance can be formulated as follows:

$$A(\lambda,t) = \varepsilon_{HbO_2}(\lambda)[HbO_2](t)L(\lambda,t) + \varepsilon_{Hb}(\lambda)[Hb](t)L(\lambda,t), \tag{50.2}$$

where $\varepsilon_{HbO_2}(\lambda)$ and $\varepsilon_{Hb}(\lambda)$ are the respective extinction coefficients of oxyhemoglobin and deoxyhemoglobin at wavelength λ [6], $[HbO_2]$ (t) and $[Hb]$ (t) are the respective concentrations of oxyhemoglobin and deoxyhemoglobin, and $L(\lambda, t)$ is the optical path length of the wavelength λ at time t. The optical path length can be expressed in terms of the source–detector separation distance as follows:

$$L(\lambda,t) = DPF(\lambda,t) \cdot d, \tag{50.3}$$

where d is the distance between the light sources and the photodetector and $DPF(\lambda, t)$ is the differential path length factor [7–9].

When scattering $S(\lambda, t)$ is assumed to be constant with respect to both wavelength and time, the differential OD value at time t can be expressed as:

$$\Delta OD(\lambda,t) = \varepsilon_{HbO_2}(\lambda)\Delta\{[HbO_2]L(\lambda,t)\} + \varepsilon_{Hb}(\lambda)\Delta\{[Hb]L(\lambda,t)\}, \tag{50.4}$$

using Eqs. (50.1) and (50.2), and the measurement of the OD value at initial time t_0.

In addition, the measurement of the differential OD value can be obtained as follows:

$$\Delta OD(\lambda,t) = \log_{10} \frac{I_{in}(\lambda,t)}{I_{out}(\lambda,t)} - \log_{10} \frac{I_{in}(\lambda,t_0)}{I_{out}(\lambda,t_0)} = \log_{10} \frac{I_{out}(\lambda,t_0)}{I_{out}(\lambda,t)}, \tag{50.5}$$

In the above, $I_{in}(\lambda, t)$ at time t is equal to $I_{in}(\lambda, t_0)$ at initial time t_0 because $I_{in}(\lambda, t)$ is kept constant during measurement.

The relationship between changes in the product of the concentration and the optical path length and the differential OD values is derived from Eqs. (50.4) and (50.5), and least squares method as follows:

$$\left({}^{t}\mathbf{AA}\right)\mathbf{C} = {}^{t}\mathbf{AM}, \text{with}\,\mathbf{A} = \begin{bmatrix} \varepsilon_{HbO_2}(735) & \varepsilon_{Hb}(735) \\ \varepsilon_{HbO_2}(810) & \varepsilon_{Hb}(810) \\ \varepsilon_{HbO_2}(850) & \varepsilon_{Hb}(850) \end{bmatrix},$$
$$\mathbf{C} = \begin{bmatrix} \Delta\{[HbO_2](t)L(t)\} \\ \Delta\{[Hb](t)L(t)\} \end{bmatrix} \text{and}\,\mathbf{M} = \begin{bmatrix} \Delta OD(735,t) \\ \Delta OD(810,t) \\ \Delta OD(850,t) \end{bmatrix}, \tag{50.6}$$

where $L(t)$ is the optical path length assuming, for simplicity, that the path length of all wavelengths are approximately equal. Changes in the product of the concentration and the optical path length, $\Delta\{[HbO_2](t)L(t)\}$ and $\Delta\{[Hb](t)L(t)\}$, can be determined by solving Eq. (50.6).

In addition, change in the product of the total hemoglobin concentration and the optical path length, $\Delta\{[tHb](t)L(t)\}$, is obtained as follows:

$$\Delta\{[tHb](t)L(t)\} = \Delta\{[HbO_2](t)L(t)\} + \Delta\{[Hb](t)L(t)\} \tag{50.7}$$

4 Evaluation

4.1 Solid Phantom Test

To evaluate the performances of our NIRS system, an epoxy based solid phantom (absorption coefficient $[\mu_a] = 0.04\,\text{mm}^{-1}$ and reduced scattering coefficient $[\mu_s'] = 0.8\,\text{mm}^{-1}$) was used. The signal-to-noise ratio (SNR) is limited by shot noise generated by the random arrival of incidence photons at the photodetector.

The solid phantom test revealed that an SNR of at least 60 dB was obtainable with our system.

4.2 Arm Cuff Occlusion Test

The ability of the PocketNIRS Duo to measure oxygenation in human subjects was evaluated using an arm cuff occlusion test. The optical probe was placed on the left forearm of the subject. The PocketNIRS Duo clearly detected changes in forearm hemodynamics following cuff occlusion at 200 mmHg for 3 min (Fig. 50.3 shows the typical plots of one subject among five subjects).

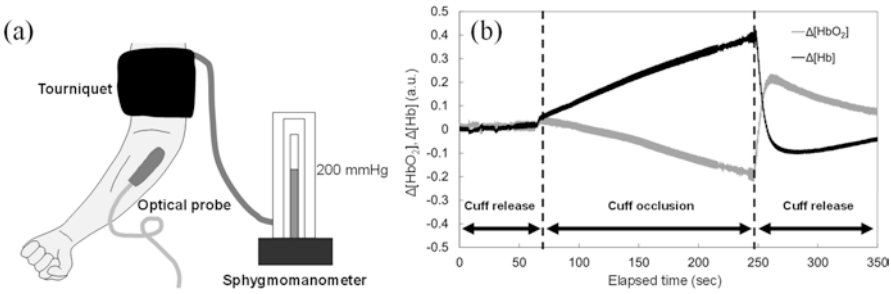

Fig. 50.3 Result of the arm cuff occlusion test (**a**) Experimental setup (**b**) Plots of changes in the product of hemoglobin concentrations and the optical path length in the left forearm of a subject

4.3 Breath-Holding Experiment

To evaluate the ability of the PocketNIRS HM to measure brain hemodynamics we performed a breath-holding experiment. The optical probe was placed on the left side of the subject's forehead and a commercial pulse-oximeter sensor (8000R, Nonin Medical Inc.), which source-detector separation was approximately 7.5 mm, was attached on the right side of the forehead. The commercial pulse-oximeter sensor (SR-5C, Konica Minolta Inc.) was attached on the right forefinger. The forehead hemodynamics and forefinger S_pO_2 (blood oxygen saturation level) data are presented in Fig. 50.4, which shows typical plots of one subject among five subjects. The subject held their breath 30 s after the commencement of measurements. In response to breath-holding, the S_pO_2 value recorded by the pulse oximeter gradually decreased. The PocketNIRS HM detected a decrease in $\Delta[HbO_2]$ and an increase in $\Delta[Hb]$ a few tens of seconds after an increase in $\Delta[HbO_2]$ and $\Delta[Hb]$. The subject restarted breathing approximately 136 s later. Following rebreathing, $\Delta[HbO_2]$ increased and $\Delta[Hb]$ decreased but the S_pO_2 of the right forehead recovered later than these signals. Especially, the recovery and the initiation of S_pO_2 in the right forefinger was delayed approximately 10 s than that in the right forehead. A small wave, the period of which is approximately 0.96 Hz (57 bpm), could be observed in $\Delta[HbO_2]$ signal, which could be attributed to the subject's heartbeat.

The PocketNIRS HM therefore demonstrates sufficient sensitivity to clearly monitor brain hemodynamics and has a data acquisition rate sufficient to detect pulsation due to heartbeat.

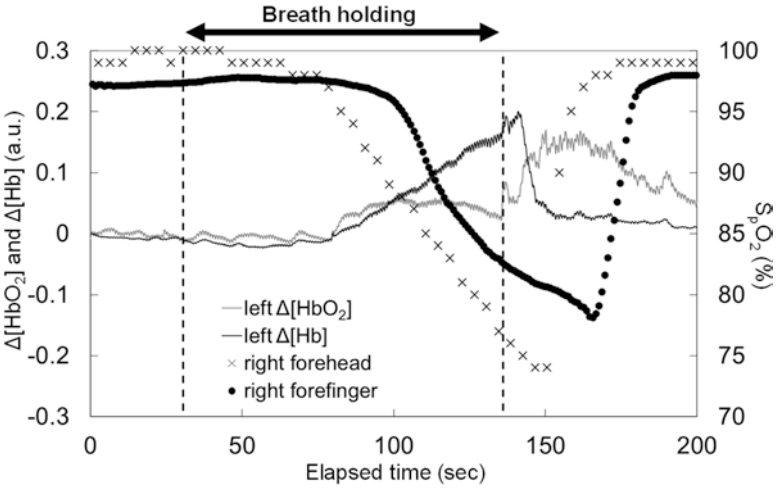

Fig. 50.4 Changes in brain oxygenation during a breath-holding experiment

5 Conclusion

We have developed a portable wireless NIRS system, the PocketNIRS Duo, and the related PocketNIRS HM system that specifically facilitates the analysis of brain hemodynamics. The primary features of these systems are their ability to measure changes in oxyhemoglobin, deoxyhemoglobin and total hemoglobin concentration. These systems demonstrate a high SNR (greater than 60 dB), fast data acquisition rate (up to 60 Hz), and simultaneous two-channel probe operation capability. Furthermore, the small size and light weight (requiring only two AAA batteries for operation), and the wireless capabilities of these systems (which are controllable by either smartphone or personal computer) make these devices ideal tools not only for clinical applications but also for healthcare monitoring at home, sports medicine, and the field of brain research.

References

1. Jöbsis FF (1977) Noninvasive, infrared monitoring of cerebral and myocardial oxygen sufficiency and circulatory parameters. Science 198:1264–1267
2. Barlow CH, Burns DH, Callis JB (1989) Breast biopsy analysis by spectroscopic imaging. In: Chance B (ed) Photon migration in tissues. Plenum Press, New York, pp 111–119
3. Wahr JA, Tremper KK, Samra S et al (1996) Near-infrared spectroscopy: theory and applications. J Cardiothoracic Vasc Anesth 10:406–418
4. Chance B, Alfano R (eds) (1997) Optical tomography and spectroscopy of tissue: theory, instrumentation, model, and human studies II. Proc SPIE 2979

5. Chance B, Alfano R, Tromberg B (eds) (1999) Optical tomography and spectroscopy of tissue: theory, instrumentation, model, and human studies III. Proc SPIE 3597
6. Cope M, Delpy DT (1988) A system for long-term measurement of cerebral blood and tissue oxygenation in newborn infants by near infrared transillumination. Med Biol Eng Comput 26:289–294
7. Delpy DT, Cope M, van der Zee P et al (1998) Estimation of optical pathlength through tissue from direct time of flight measurement. Phys Med Biol 33:1433–1442
8. Boas DA, Franceschini MA, Dunn AK et al (2002) Noninvasive imaging of cerebral activation with diffuse optical tomography. In: Frostig RD (ed) In vivo optical imaging of brain function. CRC Press, Boca Raton, pp 193–221, Chap. 8
9. Zhao H, Tanikawa Y, Gao F et al (2002) Maps of optical differential pathlength factor of human adult forehead, somatosensory motor and occipital regions at multi-wavelengths in NIR. Phys Med Biol 47:2075–2093